Since January 2020 Elsevier has created a COVID-19 resource centre with free information in English and Mandarin on the novel coronavirus COVID-19. The COVID-19 resource centre is hosted on Elsevier Connect, the company's public news and information website.

VIROLOGY 118, 345-352 (1982)

Equine Arteritis Virus-Infected Cells Contain Six Polyadenylated Virus-Specific RNAs

MARIO F. VAN BERLO, MARIAN C. HORZINEK, AND BERNARD A. M. VAN DER ZEIJST[1]

Institute of Virology, Veterinary Faculty, State University Utrecht, Yalelaan 1, 3508 TD Utrecht, The Netherlands

Received September 1, 1981; accepted December 23, 1981

The kinetics of equine arteritis virus growth and virus-specific RNA synthesis at 40° were determined in BHK-21 cells. Maximum titers of infectious virus ($\sim 10^7$ PFU/ml) were observed at 12 hr p.i., while incorporation of [^{3}H]uridine into virus-specific RNA became detectable at 4 hr p.i. and increased to reach a maximum rate at 8 hr p.i. This RNA was labeled between 2.5 and 7 hr p.i. and isolated from infected cells. About 44% bound to oligo(dT)-cellulose; this material was denatured using glyoxal and dimethyl sulfoxide and analyzed by electrophoresis in a 1% agarose-urea gel. Six virus-specific RNA species were found having the following molecular weights: 4.3×10^6 (RNA1), 1.3×10^6 (RNA2), 0.9×10^6 (RNA3), 0.7×10^6 (RNA4), 0.3×10^6 (RNA5), and 0.2×10^6 (RNA6). RNA1 comigrated with the viral genome. Artifacts caused by defective interfering particles or breakdown of RNA were excluded. Subsequently, the target sizes of the templates for the synthesis of the genome-sized RNA and the five subgenomic RNAs were determined by uv transcription mapping. Infected cells were irradiated at 6.5 hr p.i. The effect of increasing uv doses on the RNA synthesis was determined by quantitation of the individual RNAs after separation by agarose gel electrophoresis. The uv target sizes calculated for the templates for RNAs 2-5 were very close to the physical size of RNA1. The target size of the template of RNA6 was smaller (2.8×10^6 daltons), although much greater than its physical size. The data are consistent with a model in which the individual RNAs are derived from a larger precursor RNA molecule. The consequences of these findings for the taxonomy of Togaviridae are discussed.

INTRODUCTION

Equine arteritis virus (EAV) was first isolated on a horse farm in Bucyrus, Ohio (Doll *et al.*, 1957). The principal lesions in infected animals are a necrosis of the muscle cells in the small arteries (Jones *et al.*, 1957) leading to a variety of clinical symptoms. In pregnant mares abortion occurs in about 50% of the exposed animals. Serological evidence suggests that most infections take an unapparent course (see Horzinek, 1981).

Virus particles are spherical, 50-70 nm in diameter, consisting of an isometric core structure of about 35 nm surrounded by an envelope that carries typical 12 to 15-nm ring-like structures (see Horzinek, 1981; Murphy, 1980).

The genome of EAV is a single-stranded, infectious RNA with a molecular weight of 4×10^6 (Van der Zeijst *et al.*, 1975). Three virion proteins have been described, a nucleocapsid protein of 12,000 molecular weight, a 14,000 nonglycosylated envelope protein, and a 21,000 glycosylated envelope protein (Zeegers *et al.*, 1976; see also Brinton, 1980; Horzinek, 1981). On the basis of these data EAV has been classified as nonarthropod-borne member of the Togaviridae family, not belonging to one of the existing genera (Porterfield *et al.*, 1978). In this paper we describe our studies on the replication mechanism of EAV. Multiple polyadenylated virus-specific RNAs were detected in virus-infected cells and

[1] To whom reprint requests should be addressed.

0042-6822/82/060345-08$02.00/0

uv transcription mapping was used to answer questions about the transcription mechanism of these RNAs. Our studies suggest that EAV has a replication strategy completely different from that of the alphaviruses or flaviviruses, the two main genera of the family Togaviridae.

MATERIALS AND METHODS

Cells and viruses. The Bucyrus strain of EAV (Doll *et al.*, 1957) was used. The virus was plaque purified twice before virus stocks were prepared at 37° in Vero cells infected at a multiplicity of infection (m.o.i.) of 0.01. After 1 hr adsorption the inoculum was removed and 50 ml of Dulbecco's modified Eagle's medium supplemented with 10% fetal calf serum and containing penicillin (100 IU/ml) and streptomycin (100 μg/ml) (DMEM-10% FCS) was added. The virus-containing culture medium was harvested 45 hr postinfection (p.i.) when most of the cells showed cytopathology. After removal of the debris by low-speed centrifugation, the supernatant containing 2×10^8 PFU/ml was frozen and stored at −70°; it served as stock for all experiments. Vero cells were also used for plaque titration of the virus at 40° (Van Berlo *et al.*, 1980); for all other experiments BHK-21 cells were employed and to obtain a shorter one-step growth curve of about 12 hr virus was grown at 40° rather than at 37°.

Assay of virus-specific RNA synthesis. BHK-21 cells, grown on 18 × 18-mm cover slips in 35-mm tissue culture dishes, were infected or mock infected as described in the next paragraph. After adsorption 1 ml DMEM-10% FCS containing 1 μg/ml of actinomycin D (act D) was added and cultures were pulse labeled for 60 min with [5-^{3}H]uridine (10 μCi/ml, 27.8 Ci/mmol, The Radiochemical Centre, Amersham, England). The cover slips were then washed in phosphate-buffered saline (PBS), twice in 5% trichloroacetic acid and once in ether–ethanol, and the amount of [^{3}H]uridine incorporated was measured by scintillation counting.

Isolation of [^{3}H]uridine-labeled RNA from infected cells and virus. Subconfluent cultures (approximately 2×10^6 cells) of BHK-21 cells, grown in 35-mm tissue culture dishes, were infected with 0.3 ml of the seed virus suspension to give a m.o.i. of 30. The cells were prewashed with PBS containing 50 μg/ml DEAE-dextran (Pharmacia, Uppsala, Sweden). DEAE-dextran was also present in the inoculum to enhance adsorption of EAV to the cells (Hyllseth, 1969). After 1 hr the inoculum was removed and DMEM-10% FCS was added. At 2 hr p.i. the medium was replaced by 1 ml of the same medium supplemented with 1 μg/ml act D and 0.5 hr later 25 μCi [^{3}H]uridine was added. The cells were lysed at 8 hr p.i. and RNA was extracted as described previously (Spaan *et al.*, 1981). Poly(A)-containing RNA was isolated by oligo(dT)-cellulose column chromatography; RNA was dissolved in high-salt binding buffer (10 m*M* Tris (pH 7.5), 0.05% SDS, 0.5 *M* NaCl) and applied to an oligo(dT)-cellulose column. The bound RNA was eluted with 10 m*M* Tris-HCl, pH 7.5, and recovered by ethanol precipitation (Spaan *et al.*, 1981).

To prepare [^{3}H]uridine-labeled virus, infected cells were labeled with 50 μCi/ml from 2.5 to 20 hr p.i. The infectious culture medium was harvested, clarified, and 5-ml quantities were layered on top of 35-ml 20–40% (w/v) sucrose gradients, made up in TES buffer (0.02 *M* Tris-hydrochloride, 1 m*M* EDTA, 0.1 *M* NaCl, pH 7.4). The gradients were centrifuged for 18 hr at 5° at 14,000 rpm in an SW 27 rotor. Fractions were collected and trichloroacetic acid precipitable radioactivity was determined. RNA was extracted from the radioactive virus banded at a density of 1.15 g/ml, as described previously (Spaan *et al.*, 1981).

Analytical agarose gel electrophoresis. RNA samples were denatured with glyoxal and dimethyl sulfoxide and analyzed by electrophoresis in 1% agarose horizontal slab gels as described previously (Spaan *et al.*, 1981).

UV irradiation of virus-infected cells. Subconfluent cultures (approximately 2×10^7 cells) of BHK-21 cells grown in 86-mm tissue culture dishes were infected with 2 ml of a DEAE-dextran-containing virus suspension to give a m.o.i. of 20. At 5.5 hr p.i. the medium was replaced by 7

ml DMEM-10% FCS containing 1 μg/ml act D and at 6.5 hr p.i. the plates were drained and the cultures were uv irradiated for various intervals at a dose rate of 10 erg · sec $^{-1}$ · mm^2 (Jacobs *et al.*, 1981). The cells were then incubated for 30 min in 7 ml of act D-containing DMEM-10% FCS to establish a new equilibrium state of transcription. Thereafter the cells were labeled with 7 ml of the same medium containing 700 μCi [^{3}H]uridine; 30 min later the cells were phenol extracted and the RNA was ethanol precipitated and analyzed by agarose gel electrophoresis. The effect of uv irradiation on the synthesis of the virus-specific RNAs was quantitated by counting the radioactivity in each band (Jacobs *et al.*, 1981).

The data thus obtained were used to calculate the size of the transcription template of the individual RNAs according to the uv target theory. This theory can be summarized in the expression ln $(N_t/N_0) = -K \times T \times t$, where N_t is the rate of ongoing synthesis of a particular RNA species after t seconds of irradiation; N_0 is the rate of synthesis of this RNA in the unirradiated culture; T is its target size and K is a constant (for a review of the theory see Sauerbier and Hercules, 1978). K was calculated by inserting the data for RNA1 (target size 4.3×10^6) into the formula.

Counting of samples of radioactive RNA. Unless otherwise stated, samples were spotted on Whatman 3 MM filter paper disks, which were washed three times in 5% trichloroacetic acid, once in ether-ethanol, and once in ether before they were dried and counted.

RESULTS

Kinetics of Virus Growth and Viral RNA Synthesis at 40°

A one-step growth curve of EAV in BHK-21 cells was determined (Fig. 1A). Maximum titers of infectious virus (~10^7 PFU/ml), reached at 12 hr p.i., were comparable with those observed after one-step growth in Vero cells (Van Berlo *et al.*, 1980). Virus growth in cells in the presence of 1 μg/ml act D resulted in a more severe cytopathological effect; by 12 hr p.i. approximately 40% of the cells had detached from the culture vessels. We suppose that the somewhat decreased production of EAV (Fig. 1A) was due to the prolonged exposure of the cells to the drug. Viral RNA synthesis was measured by the incorporation of [^{3}H]uridine into act D-treated cells. It became detectable at 4 hr p.i. and increased to reach a maximum rate at 8 hr p.i. before it declined again (Fig. 1B).

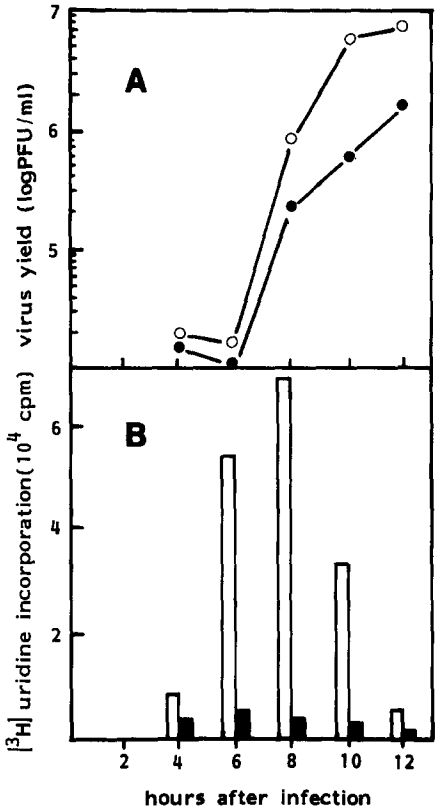

FIG. 1. Kinetics of virus growth (A) and viral RNA synthesis (B) in EAV-infected BHK-21 cells. Cells were infected with 30 PFU/cell and incubated in the absence of act D (○) or with this drug added 2 hr p.i. (●). In the latter case the kinetics of the synthesis of viral RNA were also measured by pulse labeling for 1 hr with [^{3}H]uridine at 2-hr intervals. Open bars, infected; closed bars, mock infected.

Analysis of Intracellular EAV-Specific RNA

In order to determine which species of virus-specific RNA are formed in BHK-21 cells, infected act D-treated cells were labeled with [^{3}H]uridine from 2.5 to 8 hr p.i.

At the end of this period total RNA was extracted from the cells, denatured with glyoxal and dimethyl sulfoxide, and analyzed by agarose gel electrophoresis. A number of RNA species were found in infected but not in mock-infected cells (Fig. 2, lanes A and B); they were further characterized by oligo(dT)-cellulose chromatography. Fourty-four percent of the labeled material bound to the column. This material was eluted with low salt buffer and analyzed by electrophoresis in an agarose gel. It contained six RNA species (Fig. 2, lane C). Using as markers cellular 18 S and 28 S rRNA (molecular weights 0.67×10^6 and 1.75×10^6, McMaster and Carmichael, 1977) and the intracellular Sindbis virus-specific RNAs (molecular weights 4.0×10^6 and 1.6×10^6, Simmons and Strauss, 1972) their molecular weights were determined. They were ($\times 10^6$): 4.3 (RNA1), 1.3 (RNA2), 0.9 (RNA3), 0.7 (RNA4), 0.3 (RNA5), and 0.2 (RNA6). The relative molarities of the poly(A)-containing RNA species were estimated from material labeled between 7 and 7.5 hr p.i. Two-thirds of the RNA molecules consisted of RNA5 and RNA6 (Table 1).

RNA was extracted from virus grown in replicate cultures. Only one RNA species with the same molecular weight as RNA1 was found (Fig. 2, lane D). This experiment excludes the possibility that defective (DI) particles had accumulated in our virus stocks, otherwise smaller viral RNAs would have been found. In another control experiment BHK-21 cells were infected with Sindbis virus and labeled with [^{3}H]uridine in the presence of act D between 2 and 5 hr p.i. RNA was extracted and analyzed in the same way as described for EAV intracellular RNA. Only the well-known 42 S and 26 S species (Kääriäinen and Söderlund, 1978) with no trace of degradation were found (Fig. 2, lane E). Degradation of the EAV-specific RNAs seems also unlikely since 67.5% of the polyadenylated RNA chains (at least 29.7% of the total number of RNA molecules) consisted of the RNAs 5 and 6. Since these RNAs are very small in comparison to the genome they would have been present in much lower amounts if they had originated from degradation.

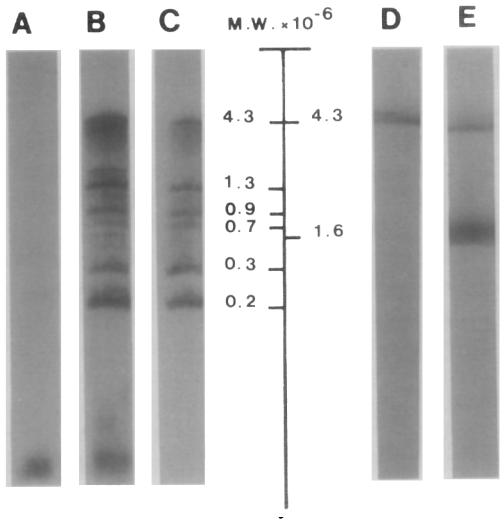

FIG. 2. Agarose gel electrophoresis of glyoxal and dimethyl sulfoxide-denatured EAV-specific intracellular RNAs. RNA was labeled with [^{3}H]uridine in the presence of act D. Material originating from about 2×10^6 mock-infected cells (A) and EAV-infected cells (B) was analyzed. Polyadenylated RNA from EAV-infected cells was purified by oligo(dT)-cellulose chromatography and electrophoresed in lane (C). Lane (D) contains RNA isolated from purified EAV. Lane (E) shows RNA from a control experiment in which cells were infected with Sindbis virus. Lanes A, B, and C are from a urea-containing gel. The other gel did not contain urea.

Effect of uv Irradiation on the Synthesis of the EAV-Specific RNAs

In order to study the mechanism by which the virus-specific subgenomic RNAs are synthesized we have used uv transcription mapping. Uv irradiation of RNA molecules induces uracil dimers; one dimer is sufficient to stop transcription of an RNA chain at that point. If repair is slow or absent the number of hits at a given dose rate will be proportional to the time of irradiation, and to the length of the template (target size) (review by Sauerbier and Hercules, 1978).

Infected cells were irradiated at 6.5 hr p.i. At this time synthesis of virus-specific RNAs is about maximal (see Fig. 1); we assume that most of the negative-stranded templates for the synthesis of the various viral RNAs have been synthesized by this time. The effect of increasing uv doses on the overall synthesis (7 to 7.5 hr p.i.) of

virus-specific RNA is shown in Fig. 3. To verify that there was no repair before or during the labeling period an experiment was done in which labeling was begun at 7.5 hr p.i., the end of the labeling period in the first experiment. There was no significant difference between the two dose-response curves, indicating that there was indeed no repair (Fig. 3).

In order to measure the exact kinetics of the inactivation of RNA synthesis by uv irradiation, it is necessary to determine the effect on the synthesis of the individual completed RNAs. Quantitation of the overall synthesis of RNA after various uv doses as depicted in Fig. 3, might lead to artifacts caused by the presence of prematurely terminated RNA molecules. Therefore, the RNAs were separated by agarose gel electrophoresis, excised from the gel, and counted. The results of a representative experiment are shown in Fig. 4. As expected on the basis of the theory, there was a linear correlation between the logarithm of the remaining RNA synthesis (N_t/N_0) and the time of uv irradiation. The slopes of the curves were about the same, indicating that the target sizes are not widely different. The target sizes for the RNAs were calculated more exactly using the numerical values for the slopes

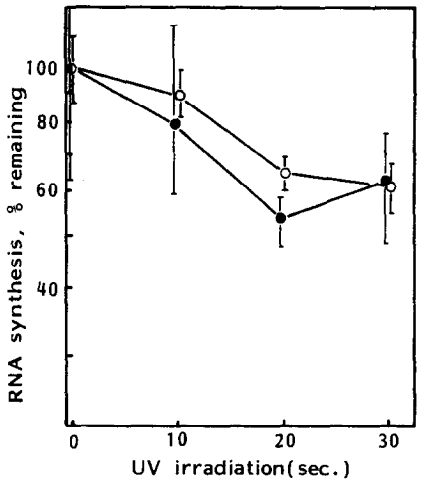

FIG. 3. Effect of uv irradiation on the overall synthesis of virus-specific RNA in EAV-infected BHK-21 cells. Infected cells grown on coverslips in 35-mm tissue culture dishes were exposed to uv irradiation at 6.5 hr p.i. for increasing periods of time. The amount of [^{3}H]uridine incorporated into trichloroacetic acid-precipitable material in the presence of act D between 7 and 7.5 hr p.i. (●) or 7.5 and 8 hr p.i. (○) was determined. After subtraction of the background in mock-infected cells (about 27% of the incorporation of the unirradiated control), the remaining virus-specific RNA synthesis at the various irradiation times was calculated. Vertical bars indicate the standard error of the mean.

of the curve in Fig. 4 obtained by linear regression analysis (Table 2). The values obtained for each of the RNAs did not correlate with the actual molecular weight but they were about equal to the molecular weight of the genome. RNAs 2 to 5 had target sizes of $4.3 \pm 0.5 \times 10^6$. The template of RNA6 had a target size of 2.8×10^6, which is smaller than that of the other RNAs; it is, however, 14 times greater than the physical size of RNA6.

TABLE 1

RELATIVE ABUNDANCE OF POLYADENYLATED VIRUS-SPECIFIC RNAS SYNTHESIZED BETWEEN 7 AND 7.5 hr p.i. IN EAV-INFECTED BHK-21 CELLS[a]

RNA	Molecular weight ($\times 10^6$)	cpm (%)	Relative molarity (%)
1	4.3	45.1	8.0
2	1.3	16.8	10.8
3	0.9	9.2	7.3
4	0.7	6.4	6.5
5	0.3	10.5	24.9
6	0.2	12.0	42.6

[a] [^{3}H]Uridine-labeled virus-specific RNA species were separated by agarose gel electrophoresis. The individual bands were excised from the gel and counted to determine the fraction of the label present in each RNA. The relative molarity of each of the RNA species was calculated.

DISCUSSION

Only recently has it been found that upon infection with coronaviruses, a family of positive-strand RNA viruses, multiple mRNAs are induced in infected cells. Six subgenomic mRNAs have been identified for mouse hepatitus virus (Spaan *et al.*, 1981; Rottier *et al.*, 1981; Wege *et al.*, 1981) and five for avian infectious bronchitis virus (Stern and Kennedy, 1980). It

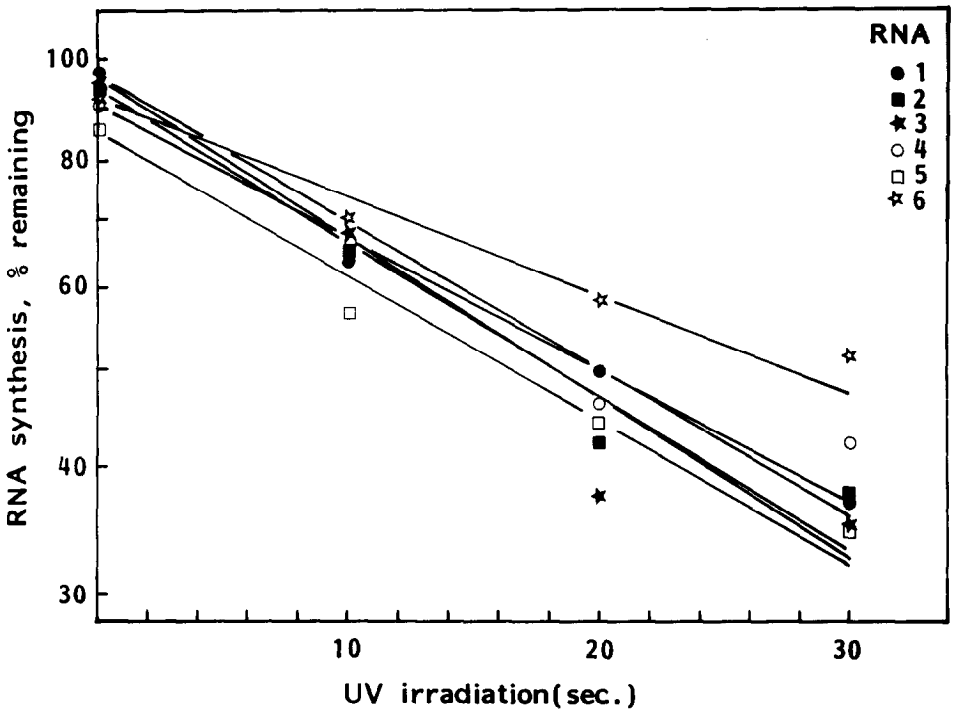

FIG. 4. Effect of increasing doses of uv irradiation on the synthesis of the individual intracellular EAV-specific RNAs. Act D-treated cells were irradiated with uv light at 6.5 hr p.i. and labeled with [^{3}H]uridine from 7 to 7.5 hr p.i. RNAs were extracted from the cells and separated by electrophoresis in an urea-containing agarose gel; RNA bands were excised from the gel, and the amount of radioactivity was determined. The graphs were fitted by linear regression analysis. The correlation coefficients (r) varied between 0.94 and 1.00.

now appears that the involvement of multiple subgenomic RNAs is not an unique feature of coronaviruses, since EAV, provisionally classified as a togavirus (Porterfield *et al.*, 1978), shows a similar pattern. However, fundamental differences seem to exist in the mode by which these RNAs are generated between coronaviruses and EAV. The results of uv transcription mapping with mouse hepatitis virus (Jacobs *et al.*, 1981) indicate that the subgenomic RNAs are synthesized via independent initiation on one or more template molecules. The uv target sizes of the templates for the EAV-specific RNAs, on the other hand, are most easily explained if we assume that the subgenomic RNAs are derived by specific cleavage or splicing from a full-length positive-stranded precursor.

Multiple mRNAs are also present in cells infected with paramyxoviruses or rhabdoviruses, but also in this case these mRNAs are synthesized by a different mechanism than the EAV subgenomic RNAs.

For vesicular stomatitis virus, e.g., cumulative target sizes for the templates of the RNAs have been found reflecting the distance of each gene to the origin of transcription (Abraham and Banerjee, 1976; Ball, 1977). This has been explained by the assumption that there is one initiation event on the genome; the completion of the genome-length positive RNA strand is not required, however, for mRNA synthesis. Alternatively vesicular stomatitis virus mRNAs could be initiated independently at different promoter sites on the genome, with subsequent elongation being dependent on the completion of promoter proximal genes (Testa *et al.*, 1980).

Addition of the molecular weights of RNAs 2 to 6 results in a value of 3.4×10^6, which is less than the molecular weight of the genome. This implies that the information in the subgenomic RNAs could be adjacent in the genome; overlapping sequences between the RNAs do not have to be postulated. We will prepare RNAs T_1 oligonucleotide fingerprints of the RNAs to answer this question. The difference between the total molecular weight of the RNAs and that of the genome may be accounted for by inaccuracies in the determination of the molecular weights or could be explained by the assumption that part of the information present in the genome is lost during the processing.

So far the only indication for the messenger nature of the RNAs 2 to 6 comes from the fact that they are polyadenylated. The main viral proteins synthesized in infected cells are the nucleocapsid protein VP1 with a molecular weight of 14,000 and the nonglycosylated envelope protein VP2 possessing a molecular weight of 19,000 (unpublished results; we consider these slightly higher molecular weights as more accurate than those described previously by Zeegers *et al.*, 1976). The molecular weights of these two proteins correspond to the coding capacity of RNAs 6 and 5, respectively, the two main virus-specific RNAs. Studies to determine the coding potential of some of the RNAs directly are in progress. More experiments are also needed to explain why RNA5 and RNA6 are synthesized in much greater molar ratios than the other RNAs.

Finally it is relevant to consider the consequences of our findings on the taxonomic status of EAV. When the Togaviridae family was officially established on the basis of morphologic criteria for the virion and the size and infectivity of the RNA (Wildy, 1971), it was already clear that it contained viruses differing considerably in ecology and antigenic properties. Initially, however, there were insufficient data to argue for or against a common origin of all togaviruses (Porterfield, 1980). As more became known about the replication mechanism of alpha- and flaviviruses, the two main genera of the togavirus family, it was argued that they were evolutionarily distinct (Cleaves *et al.*, 1981; Svitkin *et al.*, 1981).

TABLE 2

COMPARISON OF THE MOLECULAR WEIGHTS OF THE EAV-SPECIFIC INTRACELLULAR RNAS AND THE UV TARGET SIZES OF THEIR RESPECTIVE TEMPLATES

RNA	$K \times T$[a] (sec^{-1})	Daltons of RNA $\times 10^{-6}$: Target size of template[b]	Daltons of RNA $\times 10^{-6}$: RNA size[c]
1	3.22×10^{-2}	(4.3)	4.3
2	3.38×10^{-2}	4.5	1.3
3	3.60×10^{-2}	4.8	0.9
4	2.81×10^{-2}	3.8	0.7
5	3.19×10^{-2}	4.3	0.3
6	2.12×10^{-2}	2.8	0.2

[a] The value of $K \times T$ was obtained from the slope of the curves of Fig. 4 and K was calculated as 7.49×10^{-9} sec^{-1} by substituting the molecular weight of RNA1 as target size for this RNA.

[b] Using this value for K the target sizes for the other RNAs were calculated.

[c] The molecular weights of the denatured virus-specific RNAs were as determined by agarose gel electrophoresis.

Our results with EAV extend this observation and show that indeed viruses with fundamentally different replication mechanisms belong to the togavirus family. Therefore it looks as if the togavirus family as it is presently defined is a collection of positive-stranded viruses which evolved by convergent evolution to attain a similar morphologic composition.

ACKNOWLEDGMENTS

We thank Willy Spaan for his advice on the isolation and electrophoresis of RNAs and Mrs. M. Maas Geesteranus for the preparation of the manuscript.

REFERENCES

ABRAHAM, G., and BANERJEE, A. K. (1976). Sequential transcription of the genes of vesicular stomatitis virus. *Proc. Nat. Acad. Sci. USA* **73**, 1504–1508.

BALL, L. A. (1977). Transcriptional mapping of vesicular stomatitis virus in vivo. *J. Virol.* **21**, 411–414.

BRINTON, M. A. (1980). Non-arbo togaviruses. *In* "The Togaviruses: Biology, Structure and Replication" (R. W. Schlesinger, ed.), pp. 623–666. Academic Press, New York.

CLEAVES, G. R., RYAN, T. C., and SCHLESINGER,

R. W. (1981). Identification and characterization of type 2 Dengue virus replicative intermediate and replicative form RNAs. *Virology* **111**, 73–83.

DOLL, E. R., BRYANS, J. T., MCCOLLUM, W. H., and CROWE, M. E. W. (1957). Isolation of a filterable agent causing arteritis of horses and abortion by mares. Its differentiation from the equine abortion (influenza) virus. *Cornell Vet.* **47**, 3–41.

HORZINEK, M. C. (1981). "Non-arthropod-borne Togaviruses." Academic Press, London.

HYLLSETH, B. (1969). A plaque assay of equine arteritis virus in BHK-21 cells. *Arch. Ges. Virusforsch.* **28**, 26–33.

JACOBS, L., SPAAN, W. J. M., HORZINEK, M. C., and VAN DER ZEIJST, B. A. M. (1981). Synthesis of subgenomic mRNAs of mouse hepatitis virus is initiated independently: Evidence from uv transcription mapping. *J. Virol.* **39**, 401–406.

JONES, T. C., DOLL, E. R., and BRYANS, J. T. (1957). The lesions of equine viral arteritis. *Cornell Vet.* **47**, 52–68.

KÄÄRIÄINEN, L., and SÖDERLUND, H. (1978). Structure and replication of alpha-viruses. *Curr. Top. Microbiol. Immunol.* **82**, 15–69.

MCMASTER, G. K., and CARMICHAEL, G. G. (1977). Analysis of single- and double-stranded nucleic acids on polyacrylamide and agarose gels by using glyoxal and acridine orange. *Proc. Nat. Acad. Sci. USA* **74**, 4835–4838.

MURPHY, F. A. (1980). Togavirus morphology and morphogenesis. *In* "The Togaviruses: Biology, Structure and Replication" (R. W. Schlesinger, ed.), pp. 241–316. Academic Press, New York.

PORTERFIELD, J. S., CASALS, J., CHUMAKOV, M. P., GAIDAMOVICH, S. YA., HANNOUN, C., HOLMES, I. H., HORZINEK, M. C., MUSSGAY, M., OKER-BLOM, N., RUSSEL, P. K., and TRENT, D. W. (1978). Togaviridae. *Intervirology* **9**, 129–148.

PORTERFIELD, J. S. (1980). Antigenic characteristics and classification of togaviridae. *In* "The Togaviruses, Biology, Structure, Replication" (R. W. Schlesinger, ed.), pp. 13–46. Academic Press, New York.

ROTTIER, P. J. M., SPAAN, W. J. M., HORZINEK, M. C., and VAN DER ZEIJST, B. A. M. (1981). Translation of three mouse hepatitis virus strain A59 subgenomic RNAs in Xenopus laevis oocytes. *J. Virol.* **38**, 20–26.

SAUERBIER, W., and HERCULES, K. (1978). Gene and transcription unit mapping by radiation effects. *Annu. Rev. Genet.* **12**, 329–363.

SIMMONS, D. T., and STRAUSS, J. H. (1972). Replication of Sindbis virus. I. Relative size and genetic content of 26S and 49S RNA. *J. Mol. Biol.* **71**, 599–613.

SPAAN, W. J. M., ROTTIER, P. J. M., HORZINEK, M. C., and VAN DER ZEIJST, B. A. M. (1981). Isolation and identification of virus-specific mRNAs in cells infected with mouse hepatitis virus (MHV-A59). *Virology* **108**, 424–434.

STERN, D. F., and KENNEDY, S. I. T. (1980). Coronavirus multiplication strategy I. Identification and characterization of virus-specified RNA. *J. Virol.* **34**, 665–674.

SVITKIN, Y. V., UGAROVA, T. Y., CHERNOVSKAYA, T. V., LYAPUSTIN, V. N., LASHKEVICH, V. A., and AGOL, V. I. (1981). Translation of tick-borne encephalitis virus (flavivirus) genome in vitro: Synthesis of two structural polypeptides. *Virology* **110**, 26–34.

TESTA, D., CHANDA, P. K., and BANERJEE, A. K. (1980). Unique mode of transcription in vitro by vesicular stomatitis virus. *Cell* **21**, 267–275.

VAN BERLO, M. F., HORZINEK, M. C., and VAN DER ZEIJST, B. A. M. (1980). Temperature-sensitive mutants of equine arteritis virus. *J. Gen. Virol.* **49**, 97–104.

VAN DER ZEIJST, B. A. M., HORZINEK, M. C., and MOENNIG, V. (1975). The genome of equine arteritis virus. *Virology* **68**, 418–425.

WEGE, H., SIDDELL, S., STURM, M., and TER MEULEN, V. (1981). Coronavirus JHM: Characterization of intracellular virus RNA. *J. Gen. Virol.* **54**, 213–217.

WILDY, P. (1971). Classification and nomenclature of viruses. First report of the International Committee on Nomenclature of Viruses. *Monogr. Virol.* **5**, 1–81. S Karger, Basel.

ZEEGERS, J. J. W., VAN DER ZEIJST, B. A. M., and HORZINEK, M. C. (1976). The structural proteins of equine arteritis virus. *Virology* **73**, 200–205.